DESIGN AND BEAM DYNAMICS STUDIES OF A CHOPPER FOR THE JAEA-ADS LEBT

B. Yee-Rendon*, Y. Kondo, J. Tamura, F. Maekawa and S. Meigo
Japan Atomic Energy Agency (JAEA), Tokai, Japan

Abstract

The Japan Atomic Energy Agency (JAEA) designs a 30-MW CW proton linear accelerator (linac) as a key component for the accelerator-driven subcritical system (ADS) project, aimed at nuclear waste management. The low energy beam transport (LEBT) in JAEA-ADS uses charge neutralization to minimize space-charge effects, which are the primary cause of beam loss in high-power accelerators. During commissioning and power ramp-up, precise control of the duty cycle is required for safety and machine protection; thus, a chopper system will be installed to manage the beam power. The chopper is located at the LEBT, to facilitate the disposal of the excess beam power, but its operation will affect the charge neutralization producing beam transients that could lead to beam loss. To shed light on this, we created a beam optics model for the chopper using an analytic approach to determine the required characteristics like voltage and dimensions, which was confirmed through TraceWin simulations. Subsequently, we analyzed the chopper's impact on space-charge compensation to evaluate the beam transients in the LEBT. This study reports the design of the chopper and its effects on beam performance for the JAEA-ADS LEBT.

INTRODUCTION

To address the challenge of nuclear waste storage, the Japan Atomic Energy Agency (JAEA) proposes an accelerator-driven subcritical system (ADS) to transmute minor actinides [1]. JAEA-ADS is designing a 30-MW CW superconducting proton linear accelerator [2]. For high-intensity beams, space charge is a major challenge, especially at low energies. To address this issue, JAEA-ADS low energy beam transport (LEBT) adopts a space charge compensation design [3]. Space charge compensation, also referred as neutralization, occurs when the beam ionizes the residual gas. The oppositely charged particles produced by ionization accumulate in the beam potential until a steady state is reached. As a result, there is a reduction in space charge within the beam. The previous LEBT model [4] assumed a constant space-charge compensation by section. As a next step of that work, a time-dependent model that included the ionization process was created to improve the accuracy of space-charge compensation and the study of beam transients [5].

The schematic design of the new JAEA-ADS LEBT is presented in Fig. 1 (a), the design is composed of two solenoids, a chopper, and a cone collimator. The horizontal distribution along the LEBT for the transient model is shown in Fig. 1 (b). The main difference from the previous design [4], the chopper is located between the second solenoid and the conical collimator. In the present model, the chopper will be installed between the two solenoids, its final location will be decided after analyzing the chopping performance. Table 1 summarizes the main parameters of the JAEA-ADS LEBT design.

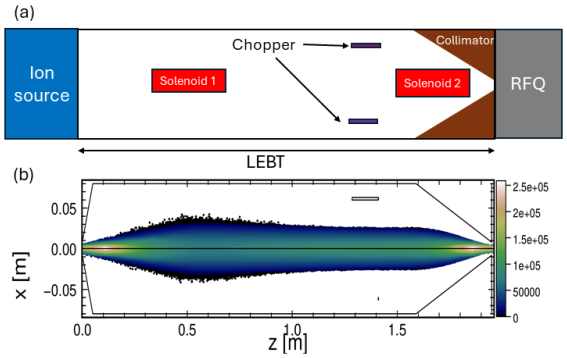

Figure 1: Schematic view of the JAEA-ADS LEBT design (a) and horizontal distribution along the LEBT (b).

Table 1: Main Parameters for the JAEA-ADS LEBT

Parameter	
Particle	Proton
Beam current (mA)	25
Beam energy (Ke) (keV)	35
Solenoid length (mm)	300
Solenoid field (mT)	191 (S1) and 243 (S2)
Length (mm)	1960

The chopper will be used to control the length of the beam pulse and thus increase the power of the beam. However, when the chopper operates, it not only kicks out the proton beam but also removes the trapped electron, destroying the space charge compensation. The beam will then require a certain amount of time to restore space charge compensation conditions. To investigate these effects, this work focuses on studying the voltage requirements of the chopper by using an analytical model, which was then compared with dynamic models of the beam, and the analysis of the transient effects of the beam current, emittance, and space-charge compensation due to the beam chopping.

* byee@post.j-parc.jp

CHOPPER

The JAEA-ADS will use an electrostatic chopper at the LEBT section to adjust the beam pulse length during the power ramping and to dump the beam in case of beam failure. Table 2 reports the design parameters for the JAEA-ADS chopper design based on modern choppers [6–8].

Table 2: Chopper Specifications

Parameter	
Type	Electrostatic
Electrode length (mm)	125
Electrode aperture (mm)	120
Voltage rise/fall time (ns)	15
Duty cycle	CW
Maximum Voltage (kV)	10

An analytical model was developed to estimate the corresponding offset and beam as a function of chopper voltage. To this, the corresponding chopper kick as a function of the chopper voltage is computed using the following expression [6]:

$$\alpha = \frac{qL_{chopper}V}{2KeD}, \tag{1}$$

where q is electric charge, $L_{chopper}$ is the chopper length, V is the voltage chopper, Ke is the kinetic energy, D is the distance between the plates.

Then, the beam offset was calculated by transporting the kick using a matrix model. The matrix transport from the chopper to the end of the LEBT, on one plane, can be represented as:

$$M_{trans} = M_{Drift2}M_{Sol}M_{Drift1}. \tag{2}$$

M_{Drift} is the matrix of a drift space:

$$M_{Drift} = \begin{bmatrix} 1 & L_{drift} \\ 0 & 1 \end{bmatrix} \tag{3}$$

where L_{drift} is the length of the drift.
M_{Sol} is the matrix of a solenoid:

$$M_{Sol} = \begin{bmatrix} cos^2(k\Delta s) & \frac{sin(k\Delta s)cos(k\Delta s)}{k} \\ ksin(k\Delta s)cos(k\Delta s) & cos^2(k\Delta s) \end{bmatrix} \tag{4}$$

where $k = \frac{B}{B\rho}$, B is the magnetic field, $B\rho$ is the beam rigidity, and Δs is the solenoid length.
The offset (Δ_R) is calculated as:

$$\begin{bmatrix} \Delta_R \\ \Delta_{R'} \end{bmatrix} = M_{trans} \begin{bmatrix} 0 \\ \alpha \end{bmatrix} \tag{5}$$

For this study two configurations are considered: Chopper A and Chopper B. Both configurations, consider the chopper between the two solenoids. For Chopper A, the chopper is located at 862.5 mm from the LEBT entrance, and Chopper B is 1347.5 mm, as shown in Fig. 2.

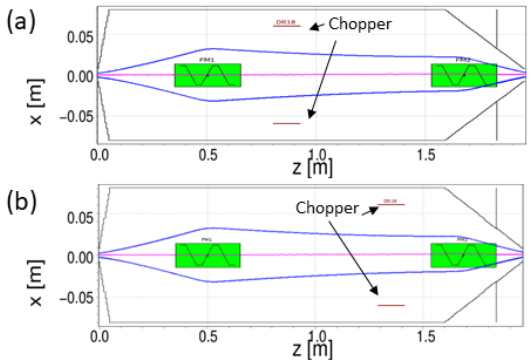

Figure 2: Two chopper positions analyzed in this study: chopper center at 862.5 mm, known as Chopper A (a), and at 1347.5 mm, called Chopper B (b).

The offset calculated from Eq. 5 provided guidelines for the chopper voltage implemented in the beam dynamic models. A comparison of the analytical model against a TraceWin model [9] is given in Fig. 3. The calculations were based on the Chopper A design, and both present a similar offset. The TraceWin model follows a linear behavior for voltages lower than 3 kV and then presents a slope, which is attributed to the effect of the beam impact with the collimator. As the beam pipe radius is 8 mm at the end of the LEBT, the minimum margin is selected as 12 mm, i.e., 1.5 × the final beam pipe radius. Multiparticle simulation carried out by TraceWin model confirmed that 3 kV does not fully dump the beam to the collimator.

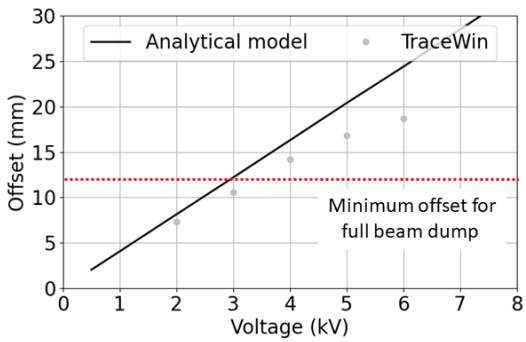

Figure 3: Comparison of the offset as a function of the chopper voltage for the analytical model and the TraceWin model.

BEAM TRANSIENT STUDIES

Transient beam studies were performed in Warp [10], a particle-in-cell program used to model high-intensity beams [11–13]. The JAEA-ADS LEBT design has been implemented in Warp to consider the ionization process and the emission of secondary electrons to simulate a more realistic space charge compensation [5].

Table 3 presents the details of the simulations. The pressure value of 1 $\times 10^{-4}$mbar was chosen to achieve a space-

Table 3: Warp simulations details. ${}^{a}\tau_{scc}$ is the space charge compensation transient time that for this simulation is 8.88 µs.

Parameter	
Beam particle	Proton
Residual gas	H_2
Smallest mesh resolution (mm)	0.5 ×0.5 ×0.5
Pressure (mbar)	1×10^{-4}
Number of macroparticles	1×10^{7}
Time step (ns)	0.1
Chopper on time (τ^{a}_{scc}/µs)	0.45/4
Simulation time (τ_{scc}/µs)	2.25/ 20

charge compensation time (τ_{scc}) of 8.88 µs to reduce the computational cost time. τ_{scc} is used in the manuscript as the unit of time because it provides more meaningful information than using an international system, which depends on pressure. However, in some cases, the corresponding value in the international system is included.

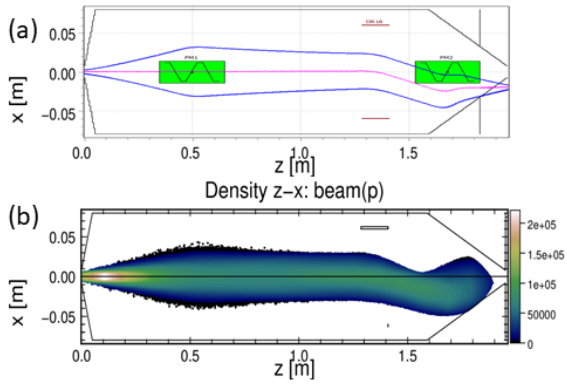

Figure 4: Comparison of the chopper performance between the TraceWin model (a) and Warp one (b).

Figure 4 compares the beam offset produced by a chopper voltage of 6 kV between the TraceWin and Warp model. There is an acceptable agreement between the features of both models. In the Warp model, the bottom electrode of the chopper does not appear, but it was simulated.

The chopper starts after the LEBT reaches the space-charge compensation steady-state, $3\tau_{scc}$. At that point, the chopper voltage increases from 0 to the rated voltage in 15 ns, and then operates at the nominal voltage for $0.45\tau_{scc}$, before decreasing back to zero in 15 ns. After this, it is simulated for another $1.88\tau_{scc}$. Figure 5 shows the transient beam currents for chopper operations, with the starting point at the beginning of the chopper ramp. The figure illustrates the behavior for 3 kV and 4 kV for the two chopper configurations. Moreover, a reference case without chopping the beam is included. A subplot provides a close-up view when the chopper is on. The results indicate that a voltage of 3 kV is insufficient to fully dump the beam. There is a time delay between the moment the chopper starts and when the effect

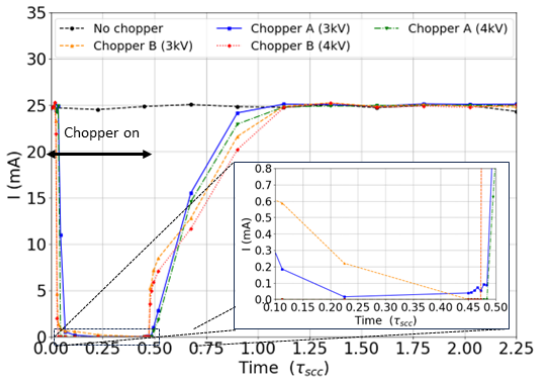

Figure 5: Comparison of the beam current evolution for the two chopper locations using 3 kV and 4 kV chopper voltage. A case without chopping the beam, No chopper, is presented as a reference. A close-up from 0.1 to $0.5\tau_{scc}$ is included.

becomes noticeable. This delay occurs because the effect propagates from the chopper position to the end, as detailed in Fig. 6. The delay is more evident for Chopper A than Chopper B because of the position of the choppers.

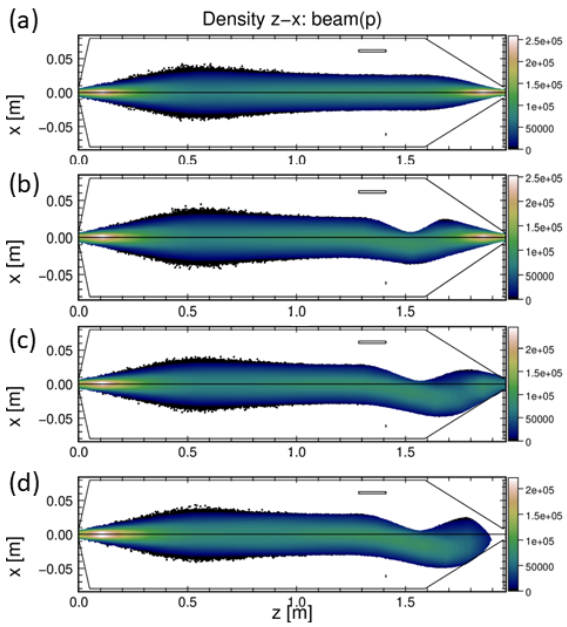

Figure 6: Chopper transients in the horizontal beam distribution for the Chopper B configuration with a voltage of 6 kV: (a) before the chopper start, (b) $0.01\tau_{scc}$, 100 ns, after the chopper started, (c) $0.02\tau_{scc}$, 200 ns, and (d) $0.03\tau_{scc}$, 250 ns. It takes about 240 ns to travel from the chopper position to the end of the LEBT.

Furthermore, Fig. 7 summarizes the beam current transients for both positions of the chopper. About $0.7\tau_{scc}$, 6 µs, is needed to restore beam current; however, Fig. 8 shows that more time ($\geq 2\tau_{scc}$) is needed to recover the steady-state emittance (black dotted line). In addition, it can be seen that the design of Chopper B, Fig. 8 (b), will take longer

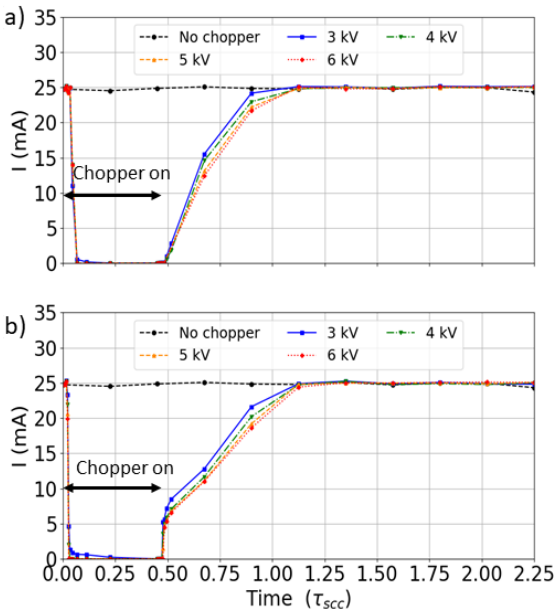

Figure 7: Beam current evolution for the Chopper A design (a) and the Chopper B (b) at different chopper voltages.

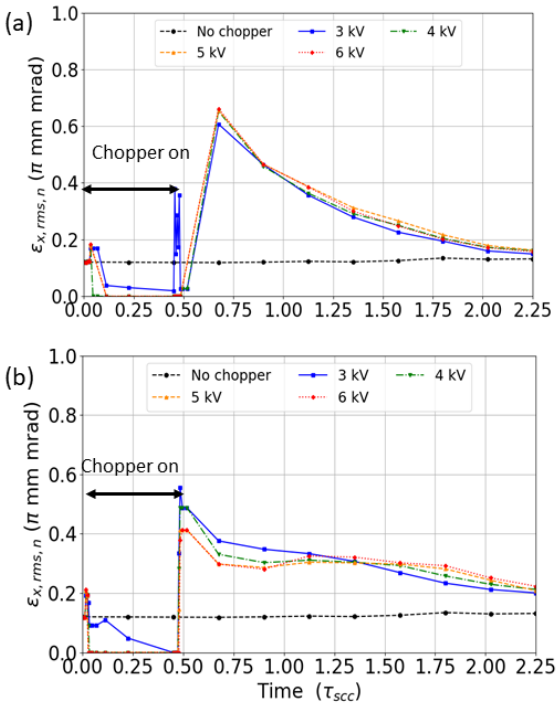

Figure 8: Emittance evolution for the Chopper A design (a) and the Chopper B (b) at different chopper voltages.

than Chopper A, Fig. 8 (a), to reach steady-state emittance. The difference is clear when comparing the SCC level at the end of the simulation as shown in Fig. 9. This is due to the significant change in electron density around the chopper. Since the chopper position in design A is further from the end of the LEBT than in design B, the electron density is less affected.

CONCLUSIONS

This study presents the initial beam dynamics investigations for the chopping operation on the JAEA-ADS linac. The calculated chopper voltages using the analytical approach agree with the results obtained from the TraceWin and Warp simulations, indicating a need for a voltage exceeding 3 kV for a complete beam dump. Warp beam transient studies assessed the chopper's performance by putting the chopper in two positions between the solenoids: after the first solenoid and before the second solenoid, with a distance difference of 485 mm. The design with a chopper after solenoid 1, Chopper design A, shows more advantages in terms of affecting less electron distribution at the end of the LEBT, therefore taking less time to recover the same condition as the steady state, about $2\tau_{scc}$. Thus, a chopper operating at 4 kV voltage, positioned at 625 mm after the LEBT entrance is capable of achieving a completed beam dump. Our next phase involves developing the electromagnetic design of the chopper to optimize its voltage and position. These findings will guide the JAEA-ADS beam power ramping up.

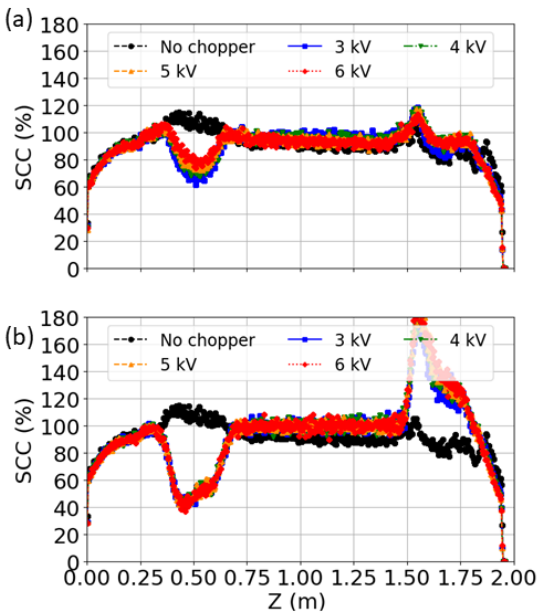

Figure 9: Space-charge compensation for the Chopper A design (a) and the Chopper B (b) at the end of the simulations for different chopper voltages.

ACKNOWLEDGMENTS

The authors thank Tomonobu Itagaki, Kai Masuda, and Nicolas Chauvin, for their valuable help with the Warp code. Kazou Hiyama, for his help installing the Warp code on the supercomputer. and Cristhian Valerio and the members of the JAEA-ADS group for their comments and suggestions. This research was conducted with the supercomputer HPE

SGI8600 in the Japan Atomic Energy Agency. This work is supported by JSPS KAKENHI Grant Number 24H00235.

REFERENCES

[1] T. Sugawara *et al.*, "Research and Development Activities for Accelerator-Driven System in Jaea", *Prog. Nucl. Energy*, vol. 106, p. 27, Feb. 2018. doi:10.1016/j.pnucene.2018.02.007

[2] B. Yee-Rendon *et al.*, "Design and beam dynamic studies of a 30-MW superconducting linac for an accelerator-driven subcritical system", *Phys. Rev. Accel. Beams.*, vol. 24, p. 120101, Dec. 2021. doi:10.1103/PhysRevAccelBeams.24.120101

[3] O. Delferrière, R. D. Duperrier, D. Uriot, N. Chauvin, R. Gobin, and P. A. P. Nghiem, "Source and Injector Design for Intense Light Ion Beams Including Space Charge Neutralisation", in *Proc. LINAC'10*, Tsukuba, Japan, Sep. 2010, paper TH302, pp. 740–744.

[4] B. Yee-Rendon *et al.*, "Design of the Low Energy Beam Transport Line for the JAEA-ADS linac", in *Proc. of the PASJ2023*, Funabashi, Japan, Aug. 2023, WEP23, pp. 545-549.

[5] B. Yee-Rendon *et al.*, "Beam Transient Studies for the JAEA-ADS LEBT", unpublished (To be presented in LINAC'24 conference).

[6] A. V. Aleksandrov, "Overview and Future Demands of Fast Choppers", in *Proc. LINAC'10*, Tsukuba, Japan, Sep. 2010, paper WE104, pp. 689–693.

[7] G. Torrisi *et al.*, "Experimental Performance of the Chopper for the ESS Linac", in *Proc. IPAC'18*, Vancouver, Canada, Apr.-May 2018, pp. 1709–1711. doi:10.18429/JACoW-IPAC2018-TUPML071

[8] I. Rodriguez, S. Lawrie, and J. Speed, "Design of an electrostatic chopper for the new ISIS MEBT", in *Proc. IPAC'23*, Venice, Italy, May 2023, pp. 2223–2226. doi:10.18429/JACoW-IPAC2023-TUPM016

[9] TraceWin Manual, http://irfu.cea.fr/dacm/logiciels

[10] A. Friedman *et al.*, "Computational methods in the WARP code framework for kinetic simulations of particle beams and plasmas", *IEEE Trans. Plasma Sci.*, vol. 42, p. 1321, June 2013. doi:10.1109/PLASMA.2013.6633427

[11] L. Bellan *et al.*, "Space Charge and Electron Confinement in High Current Low Energy Transport Lines: Experience and Simulations From IFMIF/EVEDA and ESS Commissioning", in *Proc. LINAC'22*, Liverpool, UK, Aug.-Sep. 2022, pp. 618–621. doi:10.18429/JACoW-LINAC2022-TUPORI29

[12] N. Chauvin, O. Delferriere, R. Gobin, P. A. P. Nghiem, D. Uriot, and R. D. Duperrier, "Simulations and Measurements in High Intensity LEBT with Space Charge Compensation", in *Proc. HB'12*, Beijing, China, Sep. 2012, paper THO3A03, pp. 507–510.

[13] K. Masuda *et al.*, "Commissioning of IFMIF Prototype Accelerator Towards CW Operation", in *Proc. LINAC'22*, Liverpool, UK, Aug.-Sep. 2022, pp. 319–323. doi:10.18429/JACoW-LINAC2022-TU2AA04